

Supporting Information for

A stable platinum porphyrin based photocatalyst for hydrogen production under visible light in water

Emmanouil Orfanos,^a Kalliopi Ladomenou,^{b*} Panagiotis Angaridis,^c Theodoros Papadopoulos^d
Georgios Charalambidis,^a Maria Vasilopoulou,^e Athanassios G. Coutsolelos^{a,f*}

^aUniversity of Crete, Department of Chemistry, Laboratory of Bioinorganic Chemistry, Voutes
Campus, 70013 Heraklion, Crete, Greece; E-mail: acoutsol@uoc.gr

^bInternational University of Greece, Department of chemistry, Laboratory of Inorganic Chemistry, Agios
Loucas, Kavala, 65404, Greece.

^cAristotle University of Thessaloniki, Department of General and Inorganic Chemistry, Faculty of Chemistry, GR-
54124 Thessaloniki, Greece.

^dFaculty of Science and Engineering, Thornton Science Park, University of Chester, CH2 4NU, Chester, U.K.

^eInstitute of Nanoscience and Nanotechnology, National Center for Scientific Research "Demokritos", 15341 Agia
Paraskevi, Attica, Greece.

^fInstitute of Electronic Structure and Laser (IESL) Foundation for Research and Technology - Hellas (FORTH),
Vassilika Vouton, GR 70013 Heraklion, Crete, Greece

Corresponding Authors

E-mail: acoutsol@uoc.gr (A.G.C.); kladomenou@chem.ihu.gr (K.L.); panosangaridis@chem.auth.gr (P.A.);
t.papadopoulos@chester.ac.uk (T.P.); gxaral@chemistry.uoc.gr (G.C.); manosorf17@gmail.com (E.O.)

Experimental Materials and techniques

Reagents and solvents were purchased as reagent grade from usual commercial sources and were used without further purification, unless otherwise stated. TEPP, TBPP, TPP and the metalated porphyrins were synthesized according to previously published procedures.^{4, 5} The ¹H spectra were recorded on Bruker DPX-300 MHz spectrometer using CDCl₃ as deuterated solvent with the solvent peak as the internal standard. UV-Vis absorption spectra in solution were obtained (in quartz cuvettes of 1 cm path-length) using a Shimadzu UV-1700 spectrophotometer, while the spectra in the solid state were obtained (on quartz slides 2 × 2 cm) using a UV/Vis/NIR Lambda 19, PerkinElmer spectrophotometer. SEM experiments were performed using a JEOL JSM-6390LV microscope operating at 15 and 20 kV. The samples were covered with 10 nm Au/Pd sputtering and were observed directly.

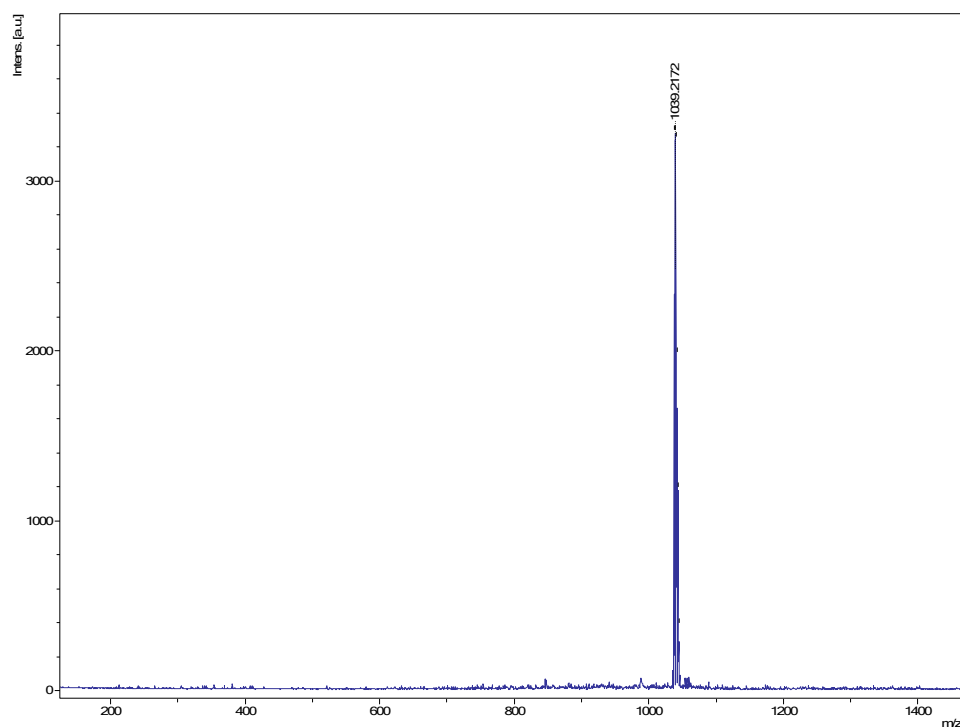


Figure S1. MALDI-TOF spectra of Pt-TEPP.

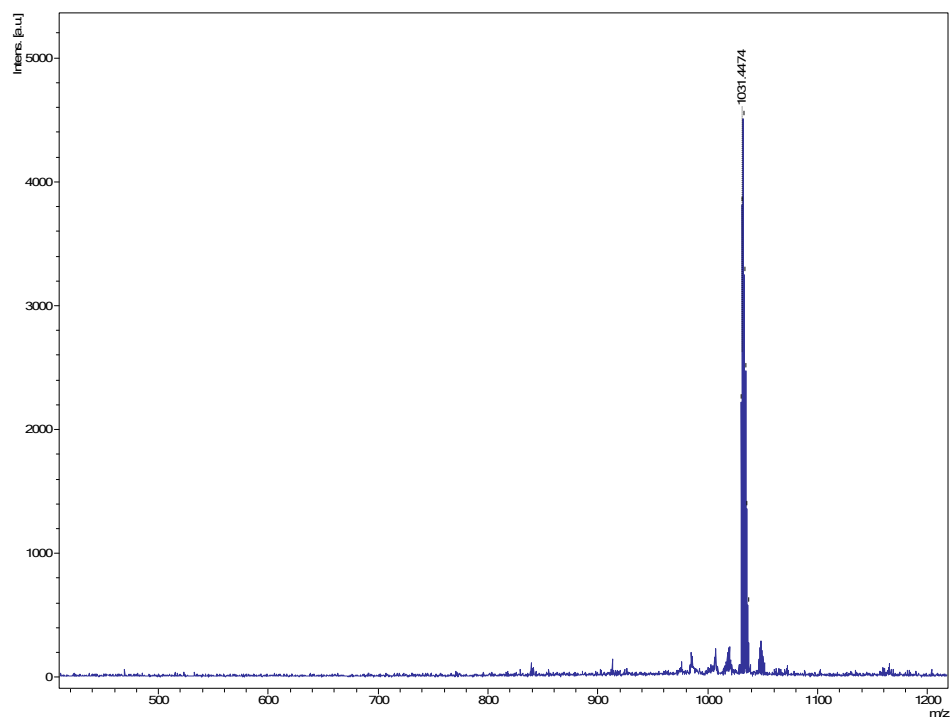


Figure S2. MALDI-TOF spectra of Pt-TBPP.

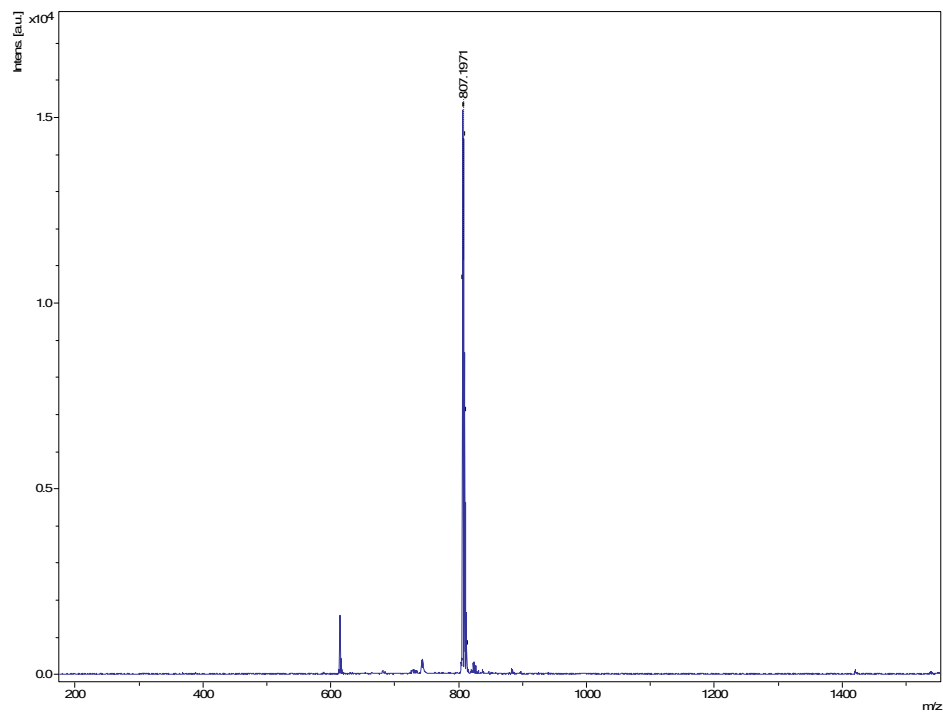


Figure S3. MALDI-TOF spectra of Pt-TPP.

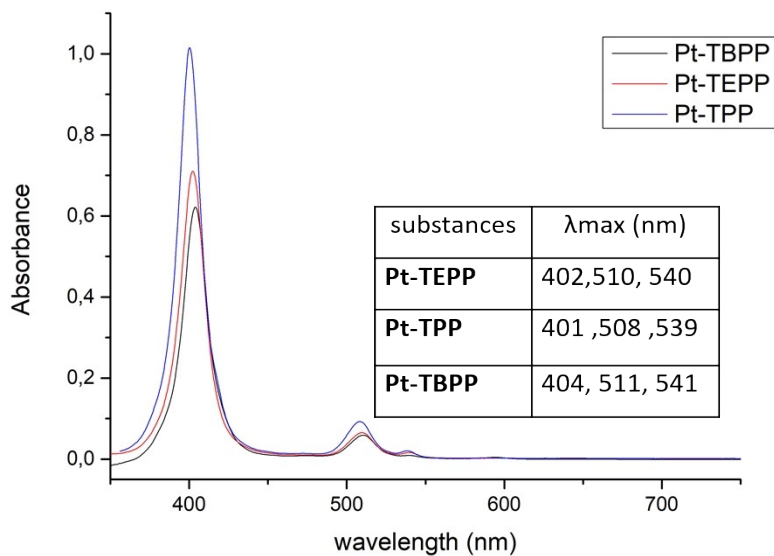


Figure S4. UV-Vis spectra of **Pt-TEPP**, **Pt-TBPP** and **Pt-TPP** photocatalysts in CH_2Cl_2 .

Single crystal X-ray diffraction analysis

Experimental

Single crystals of **Pt-TEPP** were obtained by slow evaporation of a CH_2Cl_2 /toluene solution of the compound at room temperature over a period of four weeks. A suitable crystal was selected and mounted on a STOE IPDS II diffractometer equipped with a Mo-K α sealed-tube X-ray source ($\lambda = 0.71073 \text{ \AA}$, graphite monochromated) and an image plate detector. The crystal was kept at 293(2) K during data collection. Using Olex2 1.3 [1], the structure was solved with the *SHELXS* [2] structure solution program using Direct Methods and refined with the *SHELXL* 2014/7 [3] refinement package using Least Squares minimization.

Summary of Crystal Data

Pt-TEPP. Formula $\text{C}_{52}\text{H}_{36}\text{N}_4\text{O}_8\text{Pt}$ ($M = 1,039.94 \text{ g/mol}$): monoclinic, space group P2/c (no. 13), $a = 15.432(3) \text{ \AA}$, $b = 7.2120(14) \text{ \AA}$, $c = 23.586(5) \text{ \AA}$, $\beta = 104.17(3)^\circ$, $V = 2545.1(9) \text{ \AA}^3$, $Z = 4$, $T = 293(2) \text{ K}$, $\mu(\text{MoK}\alpha) = 2.810 \text{ mm}^{-1}$, $D_{\text{calc}} = 1.357 \text{ g/cm}^3$, 4778 reflections measured ($3.562^\circ \leq 2\theta \leq 51.2^\circ$), 4778 unique ($R_{\text{int}} = 0.18$, $R_{\text{sigma}} = 0.0286$) which were used in all calculations. The final R_1 was 0.0641 ($I > 2\sigma(I)$) and wR_2 was 0.1948 (all data).

CCDC 2143453 contains the supplementary crystallographic data for **Pt-TEPP**. These data can be obtained free of charge via <http://www.ccdc.cam.ac.uk/conts/retrieving.html>, or from the Cambridge Crystallographic Data Centre, 12 Union Road, Cambridge CB2 1EZ, UK; fax: (+44) 1223-336-033; or email:deposit@ccdc.cam.ac.uk.

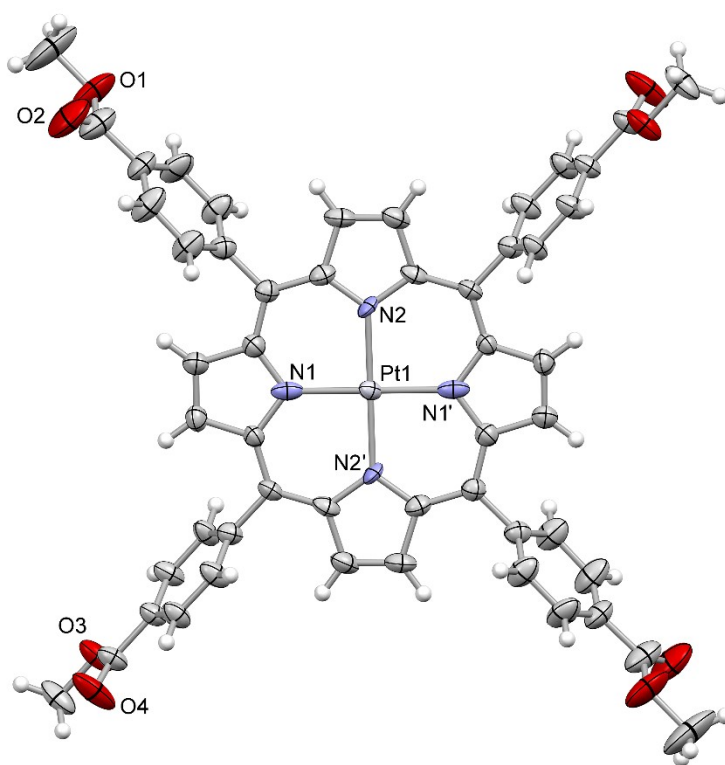


Figure S5. View of the crystal structure of **Pt-TEPP** with displacement ellipsoids shown in the 35% probability level (Color code: C atoms, dark gray ellipsoids; O atoms, red ellipsoids; N atoms, blue ellipsoids; Pt, light gray ellipsoids; H atoms, spheres of arbitrary radius).

Table S1 Crystal data and structure refinement for Pt-TEPP

Empirical formula	$C_{52}H_{36}N_4O_8Pt$
Formula weight	1,039.94
Temperature/K	293(2)
Crystal system	monoclinic
Space group	$P2_1/c$
$a/\text{\AA}$	15.432(3)
$b/\text{\AA}$	7.2120(14)
$c/\text{\AA}$	23.586(5)
$\beta/^\circ$	104.17(3)

Volume/Å ³	2545.1(9)
Z	4
$\rho_{\text{calc}}/\text{g}/\text{cm}^3$	1.357
μ/mm^{-1}	2.810
F(000)	1036.0
Crystal size/mm ³	0.7 × 0.3 × 0.05
Radiation	MoK α ($\lambda = 0.71073$)
2 θ range for data collection/°	3.562 to 51.2
Index ranges	-18 ≤ h ≤ 18, -8 ≤ k ≤ 8, -28 ≤ l ≤ 28
Reflections collected	4778
Independent reflections	4778 [$R_{\text{int}} = 0.18$, $R_{\text{sigma}} = 0.0286$]
Data/restraints/parameters	4778/0/298
Goodness-of-fit on F ²	1.056
Final R indexes [$I \geq 2\sigma(I)$]	$R_1 = 0.0641$, $wR_2 = 0.1906$
Final R indexes [all data]	$R_1 = 0.0767$, $wR_2 = 0.1948$
Largest diff. peak/hole / e Å ⁻³	1.79/-3.58

Table S2 Selected Bond Lengths for Pt-TEPP.

Atom Atom Length/Å

Pt1 N1¹ 2.007(10)

Pt1 N1 2.007(10)

Pt1 N2 2.033(7)

Pt1 N2¹ 2.033(7)

¹-X,-Y,1-Z

Table S3 Selected Bond Angles for Pt-TEPP.

Atom Atom Atom Angle/°

N1¹ Pt1 N1 180.0

N1 Pt1 N2 90.7(3)

N1 Pt1 N2¹ 89.3(3)

N1¹ Pt1 N2 89.3(3)

N1¹ Pt1 N2¹ 90.7(3)

N2 Pt1 N2¹ 180.0

¹-X,-Y,1-Z

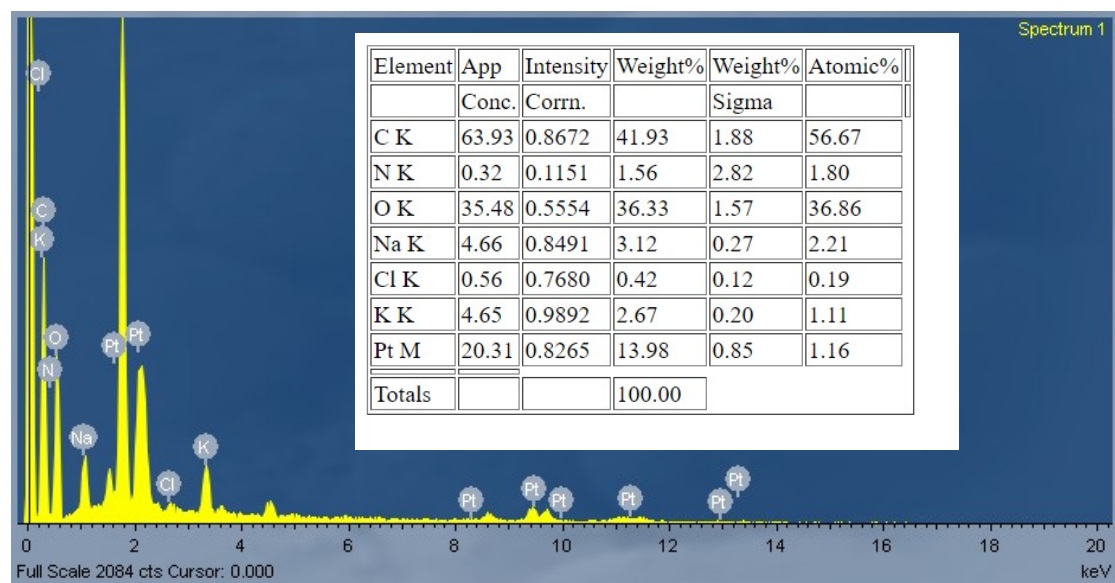


Figure S6. SEM/EDS analysis for Pt-TEPP.

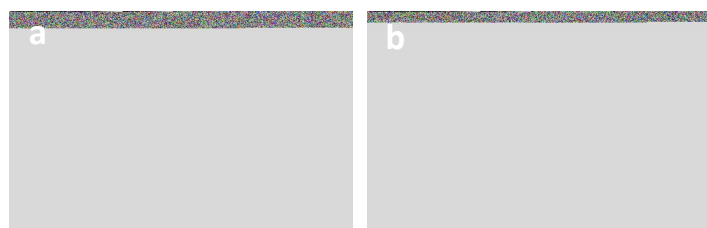


Figure S7. SEM images of photocatalysts a) **Pt-TBPP** and b) **Pt-TPP**.

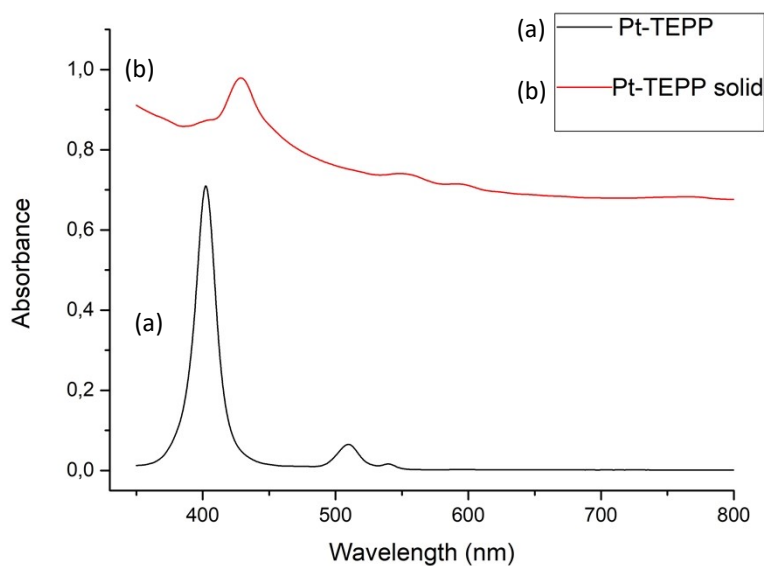


Figure S8. Absorption spectra of **Pt-TEPP** in (a) in solution (CH_2Cl_2) and (b) in solid-state.

Electrochemical Measurements

Cyclic and square wave voltammetry experiments were carried out in deionized water at room temperature using an AutoLab PGSTAT20 potentiostat in the presence of 0.1 M sodium sulfate (Na_2SO_4) solution at pH=5 as the supporting electrolyte. A three-electrode cell setup was used with platinum as the working electrode (3 mm diameter), Ag/AgCl as the reference electrode and a platinum wire as the counter electrode. Oxygen was removed by purging the aqueous solution with nitrogen. The working electrode was polished before use with 0.05 μm alumina suspension and deionized water.

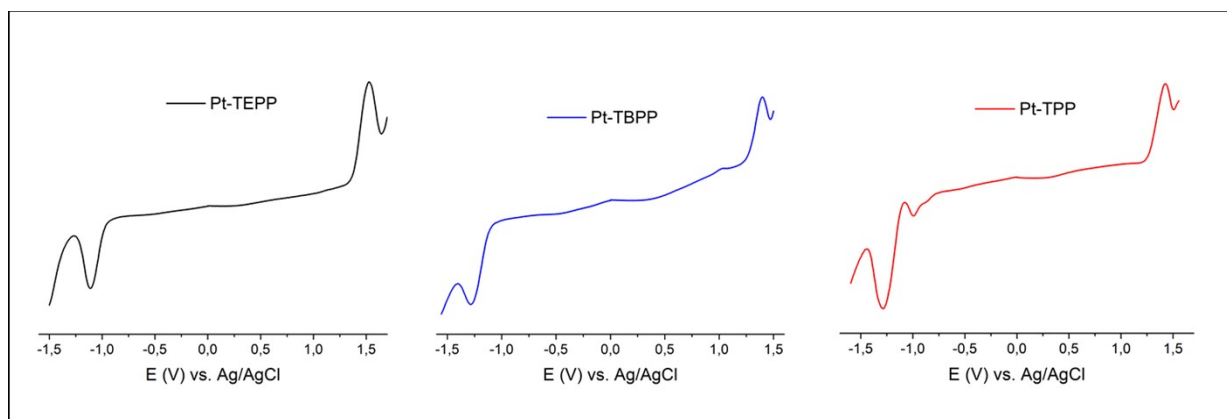


Figure S9. Square-wave voltammetry spectra of three photocatalysts **Pt-TEPP**, **Pt-TBPP** and **Pt-TPP**.

Photocatalytic measurements

The photocatalytic H₂ evolution studies were performed in a glass vial (10 mL) sealed with a rubber septum, at ambient temperature and pressure. Before each experiment, a fresh buffer solution was prepared. In detail, the solution was a 1 M aqueous solution of ascorbic acid (AA) that was adjusted to pH=4 using aqueous solution of NaOH. Initially, appropriate amount of each photocatalyst was added to the vial and then 5 ml of AA was added. Finally, the vials were sealed with a silicon septum and placed in the experimental setup where their photo-excitation took place under continuous stirring. The samples were irradiated using a low power white LED lamp ring of 40 W. The H₂ evolution was determined using gas chromatography (GC) using a Shimadzu GC 2010 plus chromatograph with a TCD detector and a molecular sieve 5 Å column (30 m - 0.53 mm). For every measurement, 100 µL were taken from the headspace of the vial and were instantly injected in the GC. In all cases, both the reported H₂ production values are the average of three independent experiments. Control experiments were performed under the same experimental conditions by removing the nanostructures or the SED from the H₂ generating systems; however, we did not detect any H₂ production.

Computational methodology

The Vienna Ab Initio Simulation Package (VASP), version 5.4.1 [6], was employed to compute the molecular dipole moment of all three porphyrin compounds using Density Functional Theory. All structures were optimized with the Perdew-Burke-Ernzerhof (PBE) gradient-corrected exchange-correlation functional [7]. Calculations were performed using plane-wave basis sets, and the projector augmented wave (PAW) method, with a plane-wave cut-off energy of 400 eV, and k-point grid of 1×1×1; one k-point is sufficient to describe isolated molecules, such as the porphyrins modelled in this work. For geometry optimization, maximum residual atomic forces were set to 0.01 eV·Å⁻¹. First-

order Methfessel-Paxton smearing with a width of 0.2 eV was used to determine how partial occupancies are set for each wave function. All compounds were modeled using a cubic cell of dimensions $a = 30 \text{ \AA}$, $b = 30 \text{ \AA}$, $c = 10 \text{ \AA}$.

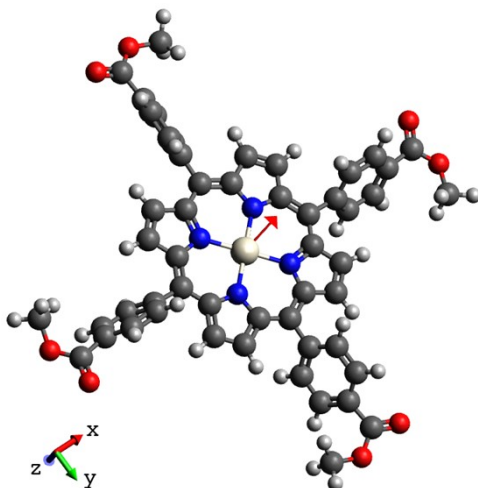


Figure S10. Illustration of the dipole moment for **Pt-TEPP** was constructed using the visualization tool Avogadro.

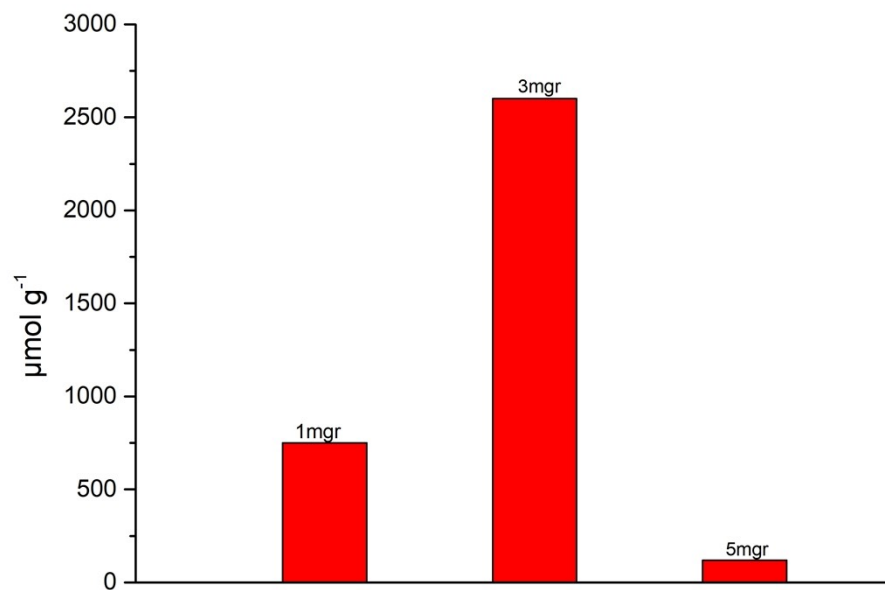


Figure S11. Photocatalytic hydrogen evolution of various amount of **Pt-TEPP** photocatalyst.

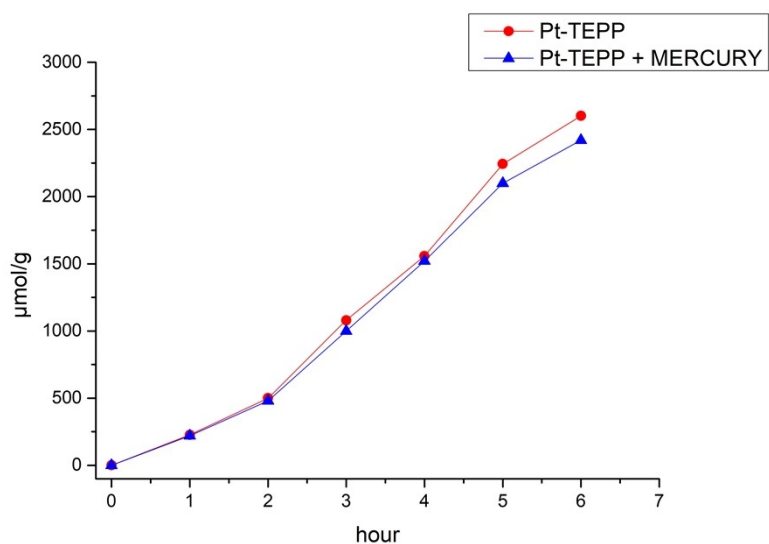


Figure S12. Hydrogen evolution of Pt-TEPP photocatalyst in aqueous solution of 1 M AA with excess mercury.

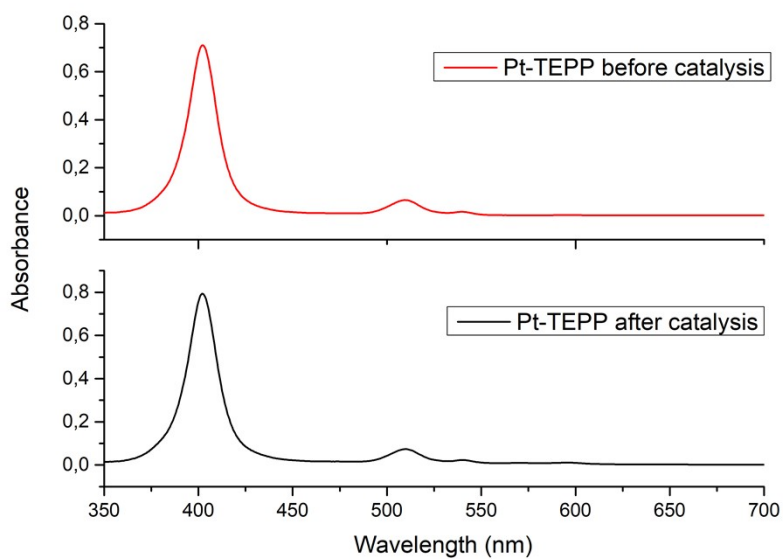


Figure S13. Absorption spectra (UV-Vis) of Pt-TEPP before (red line) and after (black line) photocatalysis in CH_2Cl_2 .

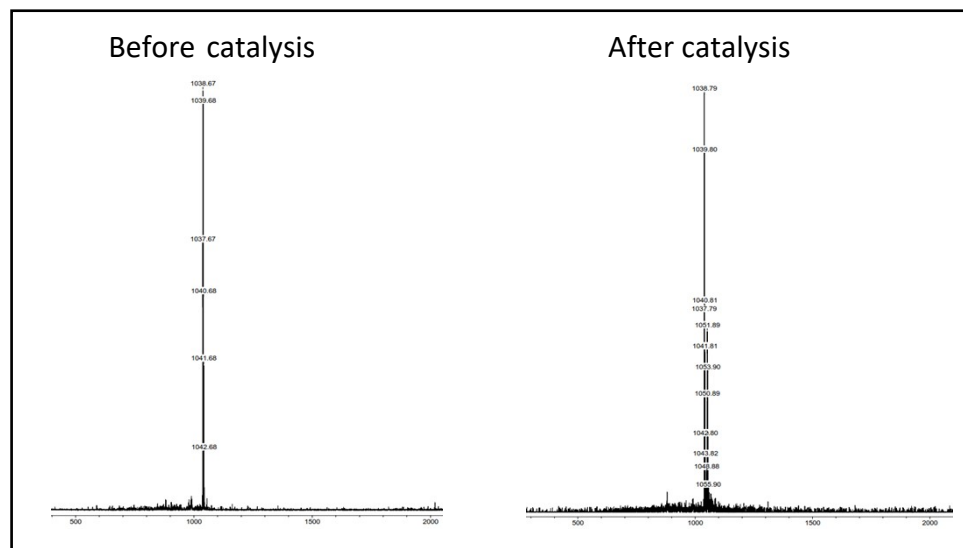


Figure S14. MALDI-TOF spectra of **Pt-TEPP** before and after photocatalysis.

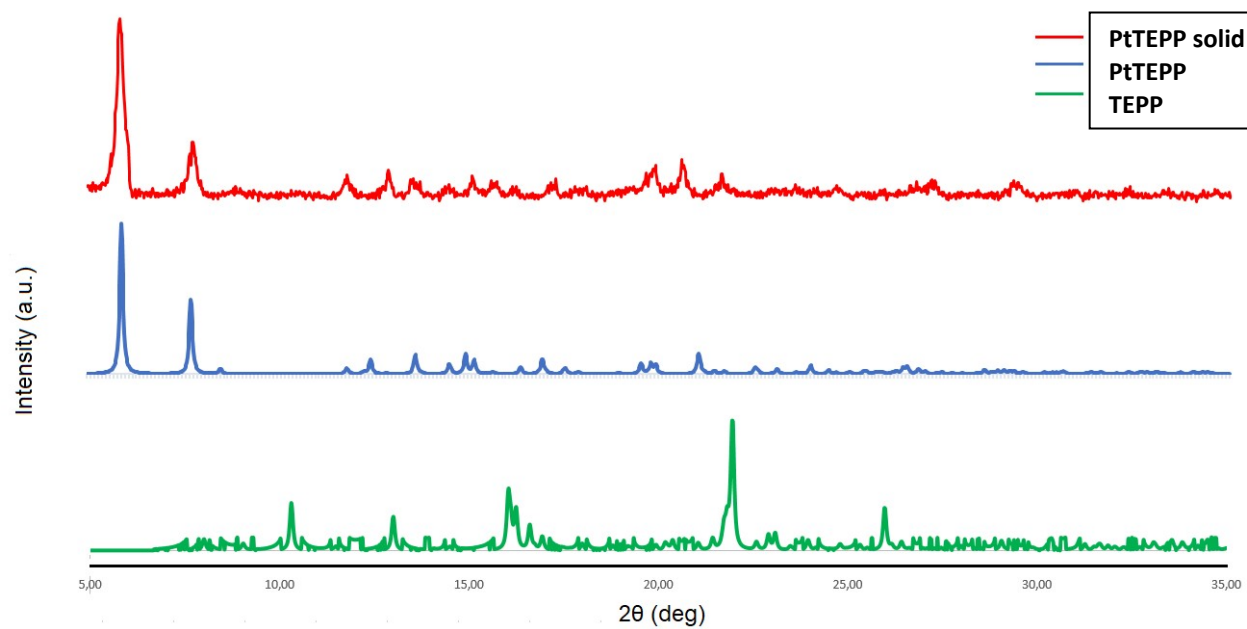


Figure S15. Powder X-ray diffraction pattern of the catalyst isolated as solid form the crude reaction mixture (**Pt-TEPP solid**) and theoretically simulated diffraction patterns from the crystal structures of **Pt-TEPP** and **TEPP**, as determined by single crystal X-ray diffraction analysis.

Table S4. Similar to our work, porphyrin based photocatalysts.

a/a	Photocatalyst	Porphyrin	Cocatalyst	Sacrificial e donor	Light	H ₂ evolution rate (μmolg ⁻¹ h ⁻¹)	References
Entry 1	Pt-TEPP	TEPP	-	Ascorbic acid	>400 nm	467.3	Our work
Entry 2	SA-TCPP	TCPP	-	Triethanolamine	>420 nm	40.8	[8]
Entry 3	PPF-Pt-Br	PPF-Br	-	Ascorbic acid	>420 nm	5390	[9]
Entry 4	Self-assembled InTPP	TPP	Pt	Ascorbic acid	>400 nm	845.4	[10]
Entry 5	Nanowires ZnTPyP	TPyP	Pt	Ascorbic acid	>420 nm	47100	[11]
Entry 6	PCN-H ₂ /Pt _{0.1}	TCPP	Pt	Triethanolamine	>400 nm	351.08	[12]
Entry 7	Octahedral ZnTPP	TPP	Pt	Ascorbic acid	>400 nm	185.5	[13]

References

1. Dolomanov, O.V., Bourhis, L.J., Gildea, R.J, Howard, J.A.K. & Puschmann, H., *J. Appl. Cryst.* 2009, **42**, 339-341.
2. Sheldrick, G. M., *Acta Cryst. A*, 2008, **64**, 112-122
3. Sheldrick, G.M., *Acta Cryst. C*, 2015, **71**, 3-8.
4. C. Stangel, D. Daphnomili, T. Lazarides, M. Drev, U. O. Krašovec and A. G. Coutsolelos, *Polyhedron*, 2013, **52**, 1016-1023.
5. H. Ghafari, S. Rahmani, R. Rahimi and E. Mohammadiyan, *RSC Advances*, 2016, **6**, 62916-62922.
6. G. Kresse, and J. Furthmüller, *Phys. Rev. B*, 1996, **54**, 11169.
7. P. Perdew, K. Burke, M. Ernzerhof, *Phys. Rev. Lett.*, 1997, **78**, 1396.
8. Z. Zhang, Y. Zhu, X. Chen, H. Zhang and J. Wang, *Advanced Materials*, 2019, **31**, 1806626.
9. X. Zhao, X. Zhang, Y. Liang, Z. Hu and F. Huang, *Macromolecules*, 2021, **54**, 4902-4909.
10. Y. Liu, L. Wang, H. Feng, X. Ren, J. Ji, F. Bai and H. Fan, *Nano Letters*, 2019, **19**, 2614-2619.
11. J. Wang, Y. Zhong, L. Wang, N. Zhang, R. Cao, K. Bian, L. Alarid, R. E. Haddad, F. Bai and H. Fan, *Nano Letters*, 2016, **16**, 6523-6528.
12. C. Lin, C. Han, H. Zhang, L. Gong, Y. Gao, H. Wang, Y. Bian, R. Li and J. Jiang, *Inorganic Chemistry*, 2021, **60**, 3988-3995.
13. A. G. Coutsolelos, P. Angaridis, E. Orfanos and K. Ladomenou, *Dalton Transactions*, 2022, DOI: 10.1039/D2DT00556E.